Title: Demographic expansion and panmixia in a St. Martin endemic, *Anolis pogus*, coincides with the decline of a competitor

Michael L. Yuan[1], Joost Merjenburgh[2], Timothy P. van Wagensveld[3], Lauren A. Esposito[1], Rayna C. Bell[1], Edward A. Myers[1]

[1]Institute for Biodiversity Science and Sustainability, California Academy of Sciences, San Francisco, California, USA

[2]Applied Biology, AERES University of Applied Science, Almere, Netherlands

[3]Reptile, Amphibian & Fish Conservation Netherlands (RAVON), Nijmegen, Netherlands

Corresponding author: Michael L Yuan (myuan@calacademy.org)

Abstract

Understanding patterns of differentiation at microgeographic scales can enhance our understanding of evolutionary dynamics and lead to the development of effective conservation strategies. In particular, high levels of landscape heterogeneity can strongly influence species abundances, genetic structure, and demographic trends. The bearded anole, *Anolis pogus*, is endemic to the topographically complex island of St. Martin and of conservation concern. Here, we examined genetic diversity and inbreeding, assessed which features of the landscape influence population abundances, tested for population genetic structure across St. Martin, and inferred historical demographic trends. We found no evidence of inbreeding or low genetic diversity in *A. pogus*. We found that suitable habitat occurs broadly across the island and that population abundances were largely predicted by canopy cover. However, there was no signature of population genetic structure across the distribution, in contrast to the co-distributed anole species (*Anolis gingivinus*). Historical demographic trends in *A. pogus* were in sharp contrast to *A. gingivinus*, with effective population sizes of *A. pogus* increasing in the recent past while *A. gingivinus* population sizes have declined. We posit that declines in a competitor species allowed for population size expansion in *A. pogus*. Overall, these analyses suggest that *A. pogus*, despite being restricted to a single island in the Lesser Antilles, is both demographically and genetically healthy. Further, we highlight the role of demographic history and ecological interactions in shaping population structure.

Keywords: Lesser Antilles, Caribbean, Fossils, abundance modeling, conservation genomics, *Anolis gingivinus*

Introduction

Islands systems have long contributed to our fundamental understanding of evolution (Grant and Grant 2011; Shaw and Gillespie 2016; Patton et al. 2021) but are also highly threatened and, thus, a focus of extensive conservation efforts (Graham et al. 2017; Russell and Kueffer 2019). Gene flow is generally strong over small spatial scales, which is thought to inhibit the formation of landscape-level variation on small islands (Wright 1943; Lenormand 2002). Consequently, species on smaller islands are often treated as singular units. Yet, a growing literature on 'microgeographic' differentiation in genetics, phenotypes, ecology, and abundance challenges this paradigm (e.g., Malhotra and Thorpe 1991; Richardson et al. 2014; Denney et al. 2020; Scotti et al. 2023; Yuan et al. 2023). Characterizing this microgeographic differentiation has implications for both our understanding of evolutionary dynamics on small islands as well as how to implement effective conservation management.

Many oceanic islands are volcanic in origin, which can generate topographically complex landscapes over short spatial distances. Variable topology can in turn lead to high degree of variation in both abiotic and biotic heterogeneity that shapes patterns of abundance, genetic structure, and demography across the landscape (Wang and Bradburd 2014; Chandler and Hepinstall-Cymerman 2016; Gurevitch et al. 2016). For example, mountainous terrain can generate population structure by inhibiting gene flow and increasing genetic drift across the landscape due to topography directly (Wright 1943; Wang 2009; Steinbauer et al. 2012; Irl et al. 2015; Verboom et al. 2015) or because of its impact on other environmental variables such as climate and habitat (Wang 2013; Wang et al. 2013; Wang and Bradburd 2014). Species that respond differently to environmental variation across the landscape are also likely to exhibit variation in local abundance (Renjifo 2001; Young and Carr 2015; Chandler and Hepinstall-

Cymerman 2016; Jesse et al. 2018). Furthermore, community composition also varies in heterogeneous landscapes leading to situations in which local abundances and population structure of a given species are shaped by the local influence of their competitors or predators (Andren 1992; Buckley and Roughgarden 2005; Kahilainen et al. 2014). Finally, islands inhabited by humans are also subject to strong land use pressure, which can alter the existing environmental landscape (Graham et al. 2017). For species with limited urban tolerance, changes in land use can lead to population declines (Selwood et al. 2015) and reduced gene flow from habitat fragmentation (Young et al. 1996; Alcaide et al. 2009; Burriel-Carranza et al. 2024). The ability for any of these environmental features to form population structure is influenced by historical demographic fluctuations which can strengthen or weaken the relative effects of genetic drift, gene flow, and selection (Slatkin and Hudson 1991; Slatkin 1993; Hutchison and Templeton 1999). Understanding how species respond to heterogeneous landscapes is vital to our understanding of evolutionary biology as well as conservation management. Integrative studies drawing from a range of ecological and genomic data can provide valuable insights into how species respond to landscape level variation.

Here, we assess landscape-level population abundance, genetic structure, and historical demography of the bearded anole, *Anolis pogus*, a species of conservation concern endemic to the island of St. Martin (Powell et al. 2020). This species presents a compelling opportunity to examine microgeographic drivers of abundance and genetic structure in a species of conservation concern. Although the island of St. Martin is only ~87 km^2, the co-distributed *Anolis gingivinus* exhibits isolation-by-distance at this scale (Jung et al. 2024) as do several other Lesser Antillean animals distributed on similarly sized islands (e.g., Malhotra and Thorpe 1991; Yuan et al. 2022; Daniel et al. 2023). Furthermore, several Lesser Antillean anoles exhibit variable abundance

81 across the landscape in relation to habitat (Buckley and Roughgarden 2005). Observational
82 reports and a limited amount of data suggests *A. pogus* abundances are higher at forested sites
83 (Lazell 1972; Schwartz and Henderson 1991; Powell et al. 2005). However, systematic
84 assessments of potential drivers of abundance variation in *A. pogus* are sparse (Jesse et al. 2018)
85 despite being fundamental for understanding the species' ecology and identifying target areas for
86 conservation. Finally, *A. pogus* and *A. gingivinus* are strong competitors (Pacala and
87 Roughgarden 1982, 1985) with *A. gingivinus* thought to be more open canopy and urban adapted
88 (Eaton et al. 2002; Powell et al. 2005). On St. Kitts and Grenada, habitat partitioning between
89 their two anole species drives differential abundances across the landscape (Buckley and
90 Roughgarden 2005). Because habitat partitioning also occurs on St. Martin with *A. pogus*
91 preferring shaded microhabitats in sympatry (Pacala and Roughgarden 1982, 1985), we expect *A.*
92 *pogus* abundances to be higher in forest habitats where competition from the more open canopy
93 adapted *A. gingivinus* should be weaker. Thus, this system also allows us to compare the effects
94 of competition and urbanization on genetic structure and demographic trends. In particular, we
95 predict that human arrival on St. Martin caused population declines in *A. pogus* due to presumed
96 deforestation (Boldingh 1909) and increased competition with the urban tolerant *A. gingivinus*.
97 Overall, our study has three main aims. First, we tested the hypothesis that *A. pogus*
98 abundances are higher in forested sites across the landscape. Second, we tested the hypothesis
99 that *A. pogus* exhibits microgeographic population structure similar to other species of Lesser
100 Antillean anoles. Third, we inferred recent demographic history in *A. pogus* and *A. gingivinus*
101 with the expectation that the former experienced recent declines due to deforestation whereas the
102 latter did not. We discuss the implications of our results for the conservation of *A. pogus* and for

our understanding of the interaction between demography and landscape-level ecology and genomics.

Methods

Abundance-based species distribution modeling

We performed abundance-based species distribution modeling using data collected from 100 plots (80 m^2) surveyed between 30 November 2018 until 08 February 2019 and distributed throughout the island of St. Martin (Fig 1B). Surveys followed the protocol of (McDiarmid et al. 2012). We also included 12 additional absence-only sites that were extensively surveyed (>2 hours) explicitly for *A. pogus* as part of our genetic samplings. We performed analyses with and without these absence-only sites to determine their influence on our results. As environmental layers, we downloaded global canopy cover (Hansen et al. 2013), mean annual temperature (BIO1) and temperature seasonality (BIO4) from WorldClim2 (Fick and Hijmans 2017), land use from WorldCover2.1 (Zanaga et al. 2022), and elevation from the Shuttle Radar Topography Mission (SRTM) (Farr and Kobrick 2000). We converted land use data into urban coverage using the proportion of cells classified as 'built-up'. All predictor rasters were resampled to 1 arc-second resolution. For distribution modeling, we extracted values from each raster layer for all survey plots.

We constructed abundance-based species distribution models using two approaches: random forest (RF) and GLM. For random forest models, we assessed variable importance as the decrease in mean squared error (MSE) and selected important variables using the *Boruta* package (Kursa and Rudnicki 2010). This method compares each variable importance with random importance generated by permuting across variables. Variables that are less important

than random are progressively dropped until only important variables remain. For our GLM approach, we first assessed dispersion using a Poisson distribution. Because our full model using a Poisson distribution was substantially over-dispersed (dispersion = 3.25), we fit our GLM using a negative binomial distribution (dispersion = 0.93). To allow more direct comparison, we refit each of our RF and GLM models using the inclusive set of variables determined as important in our RF or significant in our GLM. We used each of our refit models to predict the abundance of *A. pogus* across the landscape of St. Martin. Analyses were performed in R v4.3.2.

Whole genome sequencing

To characterize population structure and landscape genomics, we implemented a low coverage whole genome sequencing approach. Between 2018 and 2023, we sampled 54 tail tips from *A. pogus* on the island of St. Martin (Fig 2). We also included 8 samples of co-distributed *A. gingivinus* (3 from Anguilla and 5 from St. Martin) to assess comparative historical demography as described below. The population structure and landscape genetics of *A. gingivinus* on St. Martin is described elsewhere (Jung et al. 2024). We extracted whole genomic DNA from these tissues using the Qiagen DNeasy Blood & Tissue Kit. We prepared whole genome sequencing libraries using $1/4^{th}$ reactions of the NEBNext Ultra II FS DNA Library Prep Kit. We then performed 150bp paired-end sequencing on the Illumina Novaseq X platform. Following QC and adapter trimming, we aligned raw reads to the *A. sagrei* genome (AnoSag2.1; Geneva et al. 2022) using BWA-MEM (Li 2013). After removing PCR duplicates, we called SNPs in ANGSD (Korneliussen et al. 2014) retaining SNPs present in a minimum of 90% of samples, having a minimum of 108X pooled coverage, and a *P*-value less than 10^{-6}. We

148 estimated SAMtools model genotype likelihoods (Li 2011) which were incorporated into all
149 downstream genomic analyses unless otherwise stated.
150
151 *Genetic Diversity*
152 We calculated metrics of genetic diversity to assess the conservation status of *A. pogus*.
153 Using the folded SFS calculated in realSFS (Nielsen et al. 2012), we determined genome-wide
154 Tajima's D and nucleotide diversity (π) across all samples. We also assessed average inbreeding
155 coefficients (Jacquard 1974) and pairwise relatedness in ngsRelate (Korneliussen and Moltke
156 2015). Relatedness estimates were used to determine if sibling, or equivalent, pairs (i.e., $r > 0.5$)
157 were sampled which may influence our other analyses. As another estimate of potential
158 inbreeding, we assessed runs of homozygosity (ROH) using bcftools (Narasimhan et al. 2016).
159
160 *Population structure and landscape genomics*
161 We assessed overall population structure agnostic of landscape features using several
162 methods. First, we performed a principal component analysis (PCA) using genome-wide allele
163 frequencies in PCAngsd. Second, we performed multidimensional scaling (MDS) using the
164 identity-by-state (IBS) matrix generated in ANGSD. Third, we conducted admixture analyses
165 using NGSadmix for ten iterations of $K = 1$ through $K = 6$. We then selected a best K using the
166 ΔK likelihood method from (Evanno et al. 2005).
167 Next, we used landscape genomics methods to assess the effect of environmental
168 variation on genetic diversity. We then compared the relative effects of isolation-by-distance and
169 isolation-by-environment using matrix regression with randomization (MMRR) (Wang 2013).
170 Following the theoretical framework of (Hutchison and Templeton 1999), we graphically

assessed the relationship between genetic and environmental distance to determine if gene flow and genetic drift were in equilibrium using the *graph4lg* package in R (Savary et al. 2021). We calculated genomic distance as both IBS in ANGSD and raw p-distances in ngsDist (Vieira et al. 2016). We converted IBS from a similarity to a dissimilarity matrix using 1-IBS for ease of interpretation. To compare with our abundance modeling results, we selected the same set of predictor variables for tests of IBE.

Additionally, we estimated effective migration surfaces (EEMS) across the island of St. Martin (Petkova et al. 2016). This method models continuous genetic diversity across a specified landscape and is based on a stepping-stone model where migration is modeled between demes with migration rates varying by location. Using the genetic dissimilarity matrix calculated from ngsDist, we ran EEMS using a deme size of 400, with three independent starting chains for $2x10^6$ MCMC iterations following an initial burn-in of $1x10^6$ and thinning of 9,999. Posterior plots were compared across the three independent runs to ensure convergence, these three runs were then combined and visualized in the *reemsplots2* R package (https://github.com/dipetkov/reemsplots2).

Demographic modeling

To assess the demographic history of *A. pogus* and *A. gingivinus* on the island of St. Martin, we used ngsPSMC (Shchur et al. 2017). This method allowed us to incorporate genotype likelihood values into our demographic reconstruction. We estimated θ as $2N_0\mu$*bin where N_0 was 10,000, bin size was 100, and μ was 1.73×10^{-9}. Mutation rate, μ, was the average estimated rates from the genomes of six species of anoles (Kanamori et al. 2022). We set recombination rate, ρ, as 0.002 (Bourgeois et al. 2019; Moran et al. 2024). We scaled our results using a

194 generation time of 1 year (Kanamori et al. 2022). Because ngsPSMC cannot currently perform
195 bootstrapping, we assessed if demographic patterns were consistent across multiple individuals.
196 Specifically, we analyzed 6 *A. pogus* with the highest coverage (>5X) distributed across the
197 island using 20 iterations each and a PSMC pattern of 4+30*2+4+6+10 (Nadachowska-Brzyska
198 et al. 2015; Kanamori et al. 2022). For *A. gingivinus*, we analyzed 5 individuals from St. Martin
199 and 3 from Anguilla using the same parameters.
200
201 *Mitogenome analyses*
202 To compare with nuclear genomic results, we reconstructed the mitogenome for each
203 individual from our WGS data. We implemented a two-step approach to generating whole
204 reference mitogenomes. First, we aligned reads from a single individual to a whole
205 mitochondrial reference genome for *A. schwartzi* (Yuan ML, unpublished data) using BWA-
206 MEM. Both species are part of the *A. wattsi* species complex (Lazell 1972). This process yielded
207 an incomplete and non-contiguous mitochondrial genome spanning ~82% of the *A. schwartzi*
208 mitogenome. Second, we used our first pass assembly as a bait to refine the *A. pogus*
209 mitogenome (1096X coverage) for the same individual using MITObim (Hahn et al. 2013). We
210 then mapped reads for each individual to our final reference mitogenome.
211 We analyzed our mitochondrial data using consensus genotypes. These mitogenomic
212 analyses were intended to directly complement our nuclear genomic analyses described above.
213 We calculated π and Tajima's D across all samples. To assess IBD and IBE, we calculated
214 Kimura's three-parameter distance (Kimura 1981) and fit MMRR models following our genomic
215 data analyses. We estimated the mitogenome phylogeny using BEAST2 (Bouckaert et al. 2014).
216 To calculate divergence times, we implemented a random local clock using a 1.3% divergence

per million years rate estimated for vertebrate mitochondria (Macey et al. 1998), a GTR+I substitution model selected by PartitionFinder2 (Lanfear et al. 2017), and a coalescent exponential tree prior.

Results

Abundance-based species distribution modeling

Our GLM and random forest models were largely concordant with each other. We also found that models were similar whether or not additional absence-only sites were included. Thus, we only report results of our full dataset. For our random forest models, we found that urbanization, canopy cover, and elevation were important, although support for urbanization was marginal (Fig 1A). Our full random forest model explained 23.59% of variation (RMSE = 3.52). Canopy cover was the primary predictor of *A. pogus* abundance on St. Martin (MSE = 28.94%) with higher abundance in sites with more closed canopy (Fig 1A-C). Abundance was also higher in higher elevation (MSE = 17.05%) and less urbanized sites (MSE = 8.54%). In our GLM models, only canopy cover ($z = 3.28$; $P = 0.001$) and urbanization ($z = -2.55$; $P = 0.011$) were significant predictors of abundance. Specifically, *A. pogus* was more abundant in closed canopy and less urbanized sites.

Genetic Diversity

Our *A. pogus* WGS data had an averaged mapped coverage of 3.35X. Nucleotide diversity per chromosome ranged from 0.014 to 0.016. We recovered low levels of relatedness ranging from 0 to 0.095 across our sampling. Thus, we did not remove any samples for being closely related. Mean pairwise relatedness was 0.0255 ± 0.0004. Inbreeding coefficients were

240 also low across our sampling with a mean of 0.0024 ± 0.0023 and a range of 0 to 0.122. Our
241 ROH analyses are consistent with our estimated inbreeding coefficients (mean F_{ROH} = 0.0037 ±
242 0.0020). We did not find any ROH greater than 1Mbp and only 28 individuals had ROH greater
243 than 100 kbp.
244
245 *Population structure and landscape genomics*
246 Spatial clustering was not evident in our PCA, MDS, or admixture analyses (best K = 5;
247 Fig 2, S1). Consistent with these results, we found no evidence for either IBD or IBE using either
248 p-distances (MMRR: R^2 = 0.036, *P* = 0.678, Table 1) or IBS (MMRR: R^2 = 0.013, *P* = 0.830,
249 Table 1). Our graphical analyses also showed no pattern of IBD (Fig 3B). Rather, the overall
250 curve followed a case II curve which is characterized by a relatively horizontal slope with a tight
251 overall spread of genetic distances and implies a dominance of gene flow over drift (i.e.,
252 panmixia; (Hutchison and Templeton 1999). Estimated effective migration surfaces suggest that
253 the variation in gene flow across St. Martin is low (Fig S2). Regions where gene flow is
254 suggested to be reduced correspond to regions inferred to having lower abundances of *A. pogus*,
255 likely associated with lower elevation and less canopy cover in these areas (Fig 1B-C).
256
257 *Demographic modeling*
258 We found consistent support for recent population expansion in *A. pogus* among our
259 demographic analyses. Tajima's D was negative across chromosomes (range: -1.13 to -1.02). We
260 inferred consistent demographic histories from ngsPSMC across all six individuals suggesting
261 relatively robust results. We inferred two periods of major population expansion (Fig 3A). The
262 older expansion occurred during the Pleistocene from ~55–80 kya and was followed by a major

263 population decline from ~10–55 kya both during the last glacial period. The most recent
264 population expansion began during the Holocene ~2–3 kya and persists to the present. For *A.*
265 *gingivinus*, our ngsPSMC analyses inferred historical population declines from ~30–80 kya and
266 ~3000 kya to the present. We also inferred a population expansion from ~3–26 kya. Our results
267 for *A. gingivinus* were similar for the Anguilla and St. Martin populations.
268
269 *Mitochondrial comparison*
270 Mitogenome nucleotide diversity was 0.004. Consistent with our nuclear results, we
271 recovered no mitochondrial spatial structure across the island of St. Martin for *A. pogus*.
272 Specifically, we did not find evidence of either IBD or IBE (MMRR: $R^2 = 0.006$, $P = 0.951$,
273 Table 1). Our mitogenome phylogeny was well-supported but clades did not correspond to
274 populations or geographic regions (Fig 2). The last common mitochondrial ancestor of our extant
275 samples was estimated to 1.80 Ma [1.62–1.98 Ma]. As with our genomic results, our
276 mitochondrial analyses also detected signatures of a recent population expansion (Tajima's D = -
277 2.19).
278
279 **Discussion**
280 We did not find evidence of range restriction, population decline, or genetic structure in
281 *A. pogus* on the island of St. Martin. Rather, *A. pogus* was inferred to occur broadly throughout
282 the island, albeit with variable abundances primarily predicted by canopy cover. The species was
283 also inferred to be undergoing a recent demographic expansion that likely has not reached
284 equilibrium with genetic drift, resulting in panmixia. In comparison, the more widespread, urban
285 adapted (Lazell 1972; Schwartz and Henderson 1991; Eaton et al. 2002; Powell et al. 2005), and

spatially-structured (Yuan et al. 2023; Jung et al. 2024) *A. gingivinus* exhibited an unexpected signal of population decline both on St. Martin and on neighboring Anguilla. We discuss our findings and how they inform our understanding of the interaction between microgeographic adaptation, interspecific competition, and demographic responses to shared stressors in the system.

Landscape ecology and genomics

Although *A. pogus* exhibit microgeographic patterns of increased abundance with increasing canopy cover, we did not find any evidence of population structure or landscape effects in *A. pogus* for either our nuclear genomic or mitogenomic data (Fig 2, Table 1). This lack of microgeographic genomic structure may not be surprising as gene flow is expected to be stronger across short distances (Wright 1943) and St. Martin is only ~87 km^2. Yet, microgeographic population structure has been documented in several species on small islands (Richardson et al. 2014; Cheek et al. 2022). In particular, several other Lesser Antillean species display patterns of within-island microgeographic structure including other anoles (Malhotra and Thorpe 1991; Jung et al. 2024; McGreevy et al. 2024), *Setophaga plumbea* warblers (Daniel et al. 2023), and *Eleutherodactylus* whistling frogs (Yuan et al. 2022). In particular, our *A. pogus* results contrast with previous work that found IBD in *A. gingivinus* co-distributed on the island of St. Martin (Jung et al. 2024). It is possible that this difference could arise from greater dispersal propensity (i.e. stronger gene flow) in *A. pogus* compared to *A. gingivinus*. To our knowledge, the relative dispersal capabilities for these species have not yet been characterized. Alternatively, the contrasting spatial genetic patterns between *A. gingivinus* and *A. pogus* may reflect their different recent demographic histories. Notably, we recovered a signal of rapid

309 recent population growth in *A. pogus* that coincides with population decline in *A. gingivinus* (Fig
310 3A).

311 Rapid population growth following a bottleneck can result in little to no population
312 structure (Slatkin and Hudson 1991; Slatkin 1993; Milà et al. 2000; Tolley et al. 2005).
313 Following population expansion, gene flow and genetic drift are predicted to be in
314 disequilibrium. Indeed, our observed relationship between genetic and geographic distance is
315 consistent with disequilibrium between gene flow and genetic drift in which gene flow
316 predominates (Fig 3B). Furthermore, we observe a strong potential bottleneck in *A. pogus*
317 beginning during the last Pleistocene glacial period and persisting until ~3000 years ago when
318 the population began to expand (Fig 3A). By contrast, *A. gingivinus* has experienced a dramatic
319 population decline beginning around ~3000 years ago that followed a rapid population expansion
320 exiting the LGM. Because population declines reduce local genetic variation (Frankham 1996),
321 they may heighten rather than lessen population structure by increasing the effect of drift (Young
322 et al. 1996; Alcaide et al. 2009). Thus, population structure in *A. gingivinus* may be reflective of
323 either structure that has accumulated since the LGM or a result of elevated drift during recent
324 population decline. In any case, our data suggest that accounting for recent demographic
325 histories is likely important for contextualizing extant genomic structuring at a fine geographic
326 scale.

327 Although, we did not observe genetic structure in either the nuclear or mitochondrial
328 genomic datasets for *A. pogus*, we found that landscape features did predict differences in
329 relative abundances in this species across St. Martin (Fig 1). Our findings that canopy cover best
330 predicted the local abundance of *A. pogus* supports previously reported natural history
331 observations (Lazell 1972; Schwartz and Henderson 1991; Powell et al. 2005) and available

survey data (Jesse et al. 2018). On other Lesser Antillean islands with two anole species (i.e., St. Kitts and Grenada), competition suppresses local abundance beyond what would be predicted by bioenergetic models (Buckley and Roughgarden 2005). Thus, the high abundance of *A. gingivinus* in open canopy habitats (Lazell 1972; Schwartz and Henderson 1991; Eaton et al. 2002; Powell et al. 2005) likely further suppresses the population of *A. pogus* that would otherwise occur. Unfortunately, we could not directly assess the influence of competition on *A. pogus* abundances because we lacked survey data for *A. gingivinus* but our results suggest that further investigations of competition between the species may be fruitful.

Like abundances, other ecological features may also respond more rapidly than genetic structure to environmental variation following major demographic events. For example, epigenetics (Wogan et al. 2020), microbiomes (Yuan et al. 2015; Couch and Epps 2022), and morphology (Malhotra and Thorpe 1991; Yuan et al. 2023), can exhibit microgeographic variation despite a lack of concordant genomic structure. Indeed, *A. gingivinus* displays variation in dorsal coloration in response to environment that is not predicted by background population structure (Yuan et al. 2023; Jung et al. 2024). Whether this phenomenon is shared in *A. pogus* has not been formally tested. Expanding our view of these phenotypes are likely to be fruitful avenues of research for understanding landscape ecology following major demographic expansions or contractions.

Demographic response to the Anthropocene

Our demographic models indicate that population trends between *A. pogus* and *A. gingivinus* appear to be decoupled. Both species show population declines during the last glacial period. However, only *A. gingivinus* experienced demographic expansion following the LGM.

This pattern is somewhat unexpected given that total land area of St. Martin was larger during the last glacial period and subsequently shrunk throughout the Holocene. Island area effects would generally predict that carrying capacity should be higher for larger islands (Connor et al. 2000); however, other factors such as habitat suitability and competitive interactions may have greater impacts on carrying capacity than simply island size. Because we lack systematic abundance data for *A. gingivinus* and historical habitat data is limited, we cannot assess current or past habitat suitability for this species to compare with that of *A. pogus*. With respect to competition, however, fossil evidence suggests a dramatic increase in relative *A. gingivinus* abundance on Anguilla coincident with the extinction of predatory *Leiocephalus* lizards approximately 9 thousand years ago (Kemp and Hadly 2016). Thus, population expansion in *A. gingivinus* may be due to shifts in the overall community during the early Holocene.

More recently, we infer a decline in *A. gingivinus* and a population expansion in *A. pogus* following human arrival on St. Martin an estimated 5,000 years before present (Napolitano et al. 2019). *Anolis gingivinus* is thought to be better adapted to human commensal living (Powell et al. 2005) and deforestation throughout the Holocene would have increased their preferred open canopy area (Lazell 1972; Eaton et al. 2002). Correspondingly, we predicted that *A. gingivinus* should have expanded and *A. pogus* contracted during the human-occupied period. Yet, we recovered the opposite pattern. Recent work has highlighted that tolerance for urbanization does not necessarily mean species are insulated from population declines (Moran et al. 2024; Petrenko et al. 2024). Our study provides further evidence that human activity can have counterintuitive effects on species including leading to declines despite their apparent ability to inhabit urban environments.

With respect to the potential decoupling in the demographic responses of *A. gingivinus* and *A. pogus* to a shared history, one explanation is that ecological partitioning impacted how each species responded to changes in habitat distribution or overall community structure (Pacala and Roughgarden 1982). An alternative explanation is that interspecific competition drove population trends in *A. pogus*. Evidence for competition between Lesser Antillean anoles is strong and comes from both observational, modeling, and experimental data (Pacala and Roughgarden 1982, 1985; Losos 1990). We found similar recent demographic histories for *A. gingivinus* on Anguilla (where *A. pogus* is absent) and those on St. Martin (where *A. pogus* is present), suggesting that *A. gingivinus* populations are responding to broader patterns influencing the region rather than responding directly to *A. pogus* (Fig 3A). Comparatively, we argue the countervailing population trends in *A. pogus* are likely due to increased competition due to the expansion of *A. gingivinus* in the early Holocene and the subsequent decline of *A. gingivinus* following human arrival in the region.

Conservation implications

Widespread deforestation for agriculture during the colonial period (Boldingh 1909) does not appear to have had a major impact on demographic trends in *A. pogus*. Furthermore, the genomic signatures of population expansion into the present are supported by the limited available census data (Schwartz and Henderson 1991; Powell 2006). In addition to population demographic growth, overall genomic diversity appears to be strong and estimated inbreeding was extremely low. Thus, it appears that the population of *A. pogus* on St. Martin is both demographically and genetically healthy. Nevertheless, this species is restricted to a single, small island and it is clear that present abundances are substantially higher in closed canopy and higher

elevation sites (Fig 1) consistent with previous studies (Jesse et al. 2018). Overall, our data support the recent reclassification of *A. pogus* from Threatened to Near Threatened on the IUCN Red List (Powell et al. 2020). Still, long-term population stability of *A. pogus* is more likely if forested habitats are preserved given that the species occurs at lower abundances in degraded habitat including urban environments. Conservation of forested habitats should produce positive outcomes beyond *A. pogus* as deforestation appears to have broad negative impacts on many of St. Martin's other native species (Jesse et al. 2018).

Conclusion

All together, we present evidence that *A. pogus* consists of a panmictic island-wide population that is demographically and genetically healthy (Fig 2, 3B). The lack of population structure was in contrast to the co-distributed *A. gingivinus* (Jung et al. 2024). We posit that this difference is likely due to different recent demographic histories in which *A. gingivinus* has declined despite being more urban-adapted and *A. pogus* has expanded perhaps due to its declining competitor (Fig 3A). Our data show counterintuitive effects of anthropogenic activity in which the rarer species expands and the more widespread species declines.

Funding

This work was supported by an Evolutionary, Ecological, and Conservation Genomics Research Award (award number: AGA24EECG010) to MLY; and the California Academy of Sciences' Islands 2030 initiative.

Acknowledgements

All sampling was conducted under permits from the Nature Foundation Sint Maarten and Direction de L'Environnement de l'Aménagement et du Logement (DEAL) de Saint-Barthélemy et de Saint-Martin. Protocols were approved by the California Academy of Sciences and University of California, Berkeley IACUCs. We thank the Nature Foundation Sint Maarten and RAVON for sponsoring abundance survey data. For help in the field, we thank Melanie Meijer zu Schlochtern, Julien Chalifour, Leslie Hickerson, Anna Venema, Jeffrey Frederick, Catherine Jung, Laurel Allen, Lindzy Bivings, Ayanna Browne, Luigie Alequin, and Mauna Desari. For help in the lab, we thank Athena Lam and Grace Kim. Library preparation was conducted at the Center for Comparative Genomics (California Academy of Sciences) and sequencing was performed by the Vincent J. Coates Genomics Sequencing Lab (University of California, Berkeley). This study was supported by the California Academy of Sciences' Islands 2030 initiative. Additional funding was provided by an Evolutionary, Ecological, and Conservation Genomics Research Award (award number: AGA24EECG010) to MLY.

Data Availability

The following statement will be included when the manuscript is accepted by a peer reviewed journal. Raw sequence data will be accessioned in SRA. All other data will be accessioned in Dryad and code in Zenodo.

References

Alcaide, M., D. Serrano, J. J. Negro, J. L. Tella, T. Laaksonen, C. Müller, A. Gal, and E. Korpimäki. 2009. Population fragmentation leads to isolation by distance but not genetic impoverishment in the philopatric Lesser Kestrel: a comparison with the widespread and sympatric Eurasian Kestrel. Heredity 102:190–198.

Andren, H. 1992. Corvid density and nest predation in relation to forest fragmentation: a landscape perspective. Ecology 73:794–804.

Boldingh, I., 1909. *The flora of the Dutch West Indian islands St. Eustatius, Saba and St. Martin*. Brill, Leiden, Netherlands.

Bouckaert, R., J. Heled, D. Kühnert, T. Vaughan, C.-H. Wu, D. Xie, M. A. Suchard, A. Rambaut, and A. J. Drummond. 2014. BEAST 2: a software platform for Bayesian evolutionary analysis. PLOS Comput. Biol. 10:e1003537.

Bourgeois, Y., R. P. Ruggiero, J. D. Manthey, and S. Boissinot. 2019. Recent secondary contacts, linked selection, and variable recombination rates shape genomic diversity in the model species *Anolis carolinensis*. Genome Biol. Evol. 11:2009–2022.

Buckley, L. B., and J. Roughgarden. 2005. Effect of species interactions on landscape abundance patterns. J. Anim. Ecol. 74:1182–1194.

Burriel-Carranza, B., G. Mochales-Riaño, A. Talavera, J. Els, M. Estarellas, S. Al Saadi, J. D. Urriago Suarez, P. O. Olsson, M. Matschiner, and S. Carranza. 2024. Clinging on the brink: whole genomes reveal human-induced population declines and severe inbreeding in the critically endangered Emirati leaf-toed gecko (*Asaccus caudivolvulus*). Mol. Ecol. 33:e17451.

Chandler, R., and J. Hepinstall-Cymerman. 2016. Estimating the spatial scales of landscape effects on abundance. Landsc. Ecol. 31:1383–1394.

Cheek, R. G., B. R. Forester, P. E. Salerno, D. R. Trumbo, K. M. Langin, N. Chen, T. Scott Sillett, S. A. Morrison, C. K. Ghalambor, and W. Chris Funk. 2022. Habitat-linked genetic variation supports microgeographic adaptive divergence in an island-endemic bird species. Mol. Ecol. 31:2830–2846.

Connor, E. F., A. C. Courtney, and J. M. Yoder. 2000. Individuals–area relationships: the relationship between animal population density and area. Ecology 81:734–748.

Couch, C. E., and C. W. Epps. 2022. Host, microbiome, and complex space: applying population and landscape genetic approaches to gut microbiome research in wild populations. J. Hered. 113:221–234.

Daniel, A., P. Savary, J.-C. Foltête, A. Khimoun, B. Faivre, A. Ollivier, C. Éraud, H. Moal, G. Vuidel, and S. Garnier. 2023. Validating graph-based connectivity models with independent presence–absence and genetic data sets. Conserv. Biol. 37:e14047.

Denney, D. A., M. I. Jameel, J. B. Bemmels, M. E. Rochford, and J. T. Anderson. 2020. Small spaces, big impacts: contributions of micro-environmental variation to population persistence under climate change. AoB PLANTS 12:plaa005.

Eaton, J. M., S. C. Larimer, K. G. Howard, R. Powell, and J. S. Parmerlee. 2002. Population densities and ecological release of the solitary lizard Anolis gingivinus in Anguilla, West Indies. Caribb. J. Sci. 38:27–36.

Evanno, G., S. Regnaut, and J. Goudet. 2005. Detecting the number of clusters of individuals using the software structure: a simulation study. Mol. Ecol. 14:2611–2620.

Farr, T. G., and M. Kobrick. 2000. Shuttle radar topography mission produces a wealth of data. Eos Trans. Am. Geophys. Union 81:583–585.

Fick, S. E., and R. J. Hijmans. 2017. WorldClim 2: new 1-km spatial resolution climate surfaces for global land areas. Int. J. Climatol. 37:4302–4315.

Frankham, R. 1996. Relationship of genetic variation to population size in wildlife. Conserv. Biol. 10:1500–1508.

Geneva, A. J., S. Park, D. G. Bock, P. L. H. de Mello, F. Sarigol, M. Tollis, C. M. Donihue, R. G. Reynolds, N. Feiner, A. M. Rasys, J. D. Lauderdale, S. G. Minchey, A. J. Alcala, C. R. Infante, J. J. Kolbe, D. Schluter, D. B. Menke, and J. B. Losos. 2022. Chromosome-scale genome assembly of the brown anole (*Anolis sagrei*), an emerging model species. Commun. Biol. 5:1–13.

Graham, N. R., D. S. Gruner, J. Y. Lim, and R. G. Gillespie. 2017. Island ecology and evolution: challenges in the Anthropocene. Environ. Conserv. 44:323–335.

Grant, P., and B. R. Grant. 2011. How and Why Species Multiply. Princeton University Press.

Gurevitch, J., G. A. Fox, N. L. Fowler, and C. H. Graham. 2016. Landscape demography: population change and its drivers across spatial scales. Q. Rev. Biol. 91:459–485.

Hahn, C., L. Bachmann, and B. Chevreux. 2013. Reconstructing mitochondrial genomes directly from genomic next-generation sequencing reads—a baiting and iterative mapping approach. Nucleic Acids Res. 41:e129.

Hansen, M. C., P. V. Potapov, R. Moore, M. Hancher, S. A. Turubanova, A. Tyukavina, D. Thau, S. V. Stehman, S. J. Goetz, T. R. Loveland, A. Kommareddy, A. Egorov, L. Chini, C. O. Justice, and J. R. G. Townshend. 2013. High-resolution global maps of 21st-century forest cover change. Science 342:850–853.

510 Hutchison, D. W., and A. R. Templeton. 1999. Correlation of pairwise genetic and geographic
511 distance measures: inferring the relative influences of gene flow and drift on the
512 distribution of genetic variability. Evolution 53:1898–1914.
513 Irl, S. D. H., D. E. V. Harter, M. J. Steinbauer, D. G. Puyol, J. M. Fernández-Palacios, A.
514 Jentsch, and C. Beierkuhnlein. 2015. Climate vs. topography – spatial patterns of plant
515 species diversity and endemism on a high-elevation island. J. Ecol. 103:1621–1633.
516 Jacquard, A. 1974. The Genetic Structure of Populations. Springer, Berlin, Heidelberg.
517 Jesse, W. A. M., J. E. Behm, M. R. Helmus, and J. Ellers. 2018. Human land use promotes the
518 abundance and diversity of exotic species on Caribbean islands. Glob. Change Biol.
519 24:4784–4796.
520 Jung, C., J. H. Frederick, N. R. Graham, I. J. Wang, C. Fenton, K. de Queiroz, R. C. Bell, and M.
521 L. Yuan. 2024. Environmentally associated colour divergence does not coincide with
522 population structure across Lesser Antillean anoles. Biol. J. Linn. Soc. blae047.
523 Kahilainen, A., I. Keränen, K. Kuitunen, J. S. Kotiaho, and K. E. Knott. 2014. Interspecific
524 interactions influence contrasting spatial genetic structures in two closely related
525 damselfly species. Mol. Ecol. 23:4976–4988.
526 Kanamori, S., L. M. Díaz, A. Cádiz, K. Yamaguchi, S. Shigenobu, and M. Kawata. 2022. Draft
527 genome of six Cuban *Anolis* lizards and insights into genetic changes during their
528 diversification. BMC Ecol. Evol. 22:129.
529 Kemp, M. E., and E. A. Hadly. 2016. Early Holocene turnover, followed by stability, in a
530 Caribbean lizard assemblage. Quat. Res. 85:255–261.
531 Kimura, M. 1981. Estimation of evolutionary distances between homologous nucleotide
532 sequences. Proc. Natl. Acad. Sci. 78:454–458.

533 Korneliussen, T. S., A. Albrechtsen, and R. Nielsen. 2014. ANGSD: Analysis of Next
534 Generation Sequencing Data. BMC Bioinformatics 15:356.
535 Korneliussen, T. S., and I. Moltke. 2015. NgsRelate: a software tool for estimating pairwise
536 relatedness from next-generation sequencing data. Bioinformatics 31:4009–4011.
537 Kursa, M. B., and W. R. Rudnicki. 2010. Feature selection with the boruta package. J. Stat.
538 Softw. 36:1–13.
539 Lanfear, R., P. B. Frandsen, A. M. Wright, T. Senfeld, and B. Calcott. 2017. PartitionFinder 2:
540 new methods for selecting partitioned models of evolution for molecular and
541 morphological phylogenetic analyses. Mol. Biol. Evol. 34:772–773.
542 Lazell, J. D. 1972. The anoles (Sauria, Iguanidae) of the Lesser Antilles. Bull. Mus. Comp. Zool.
543 143:1–115.
544 Lenormand, T. 2002. Gene flow and the limits to natural selection. Trends Ecol. Evol. 17:183–
545 189.
546 Li, H. 2011. A statistical framework for SNP calling, mutation discovery, association mapping
547 and population genetical parameter estimation from sequencing data. Bioinformatics
548 27:2987–2993.
549 Li, H. 2013. Aligning sequence reads, clone sequences and assembly contigs with BWA-MEM.
550 ArXiv13033997 Q-Bio.
551 Losos, J. B. 1990. A phylogenetic analysis of character displacement in Caribbean *Anolis* lizards.
552 Evolution 44:558–569.
553 Macey, J. R., J. A. Schulte, A. Larson, Z. Fang, Y. Wang, B. S. Tuniyev, and T. J. Papenfuss.
554 1998. Phylogenetic relationships of toads in the *Bufo bufo* species group from the eastern

escarpment of the Tibetan plateau: a case of vicariance and dispersal. Mol. Phylogenet. Evol. 9:80–87.

Malhotra, A., and R. S. Thorpe. 1991. Microgeographic variation in *Anolis oculatus*, on the island of Dominica, West Indies. J. Evol. Biol. 4:321–335.

McDiarmid, R. W., M. S. Foster, C. Guyer, J. W. Gibbons, and N. Chernoff (eds). 2012. Reptile Biodiversity: Standard Methods for Inventory and Monitoring.

McGreevy, T.J., N.G. Crawford, P. Legreneur, C.J. Schneider. 2024. Influence of geographic isolation and the environment on gene flow among phenotypically diverse lizards. Heredity

Milà, B., D. J. Girman, M. Kimura, and T. B. Smith. 2000. Genetic evidence for the effect of a postglacial population expansion on the phylogeography of a North American songbird. Proc. R. Soc. Lond. B 267:1033–1040. Royal Society.

Moran, P. A., M. Bosse, J. Mariën, and W. Halfwerk. 2024. Genomic footprints of (pre) colonialism: population declines in urban and forest túngara frogs coincident with historical human activity. Mol. Ecol. 33:e17258.

Nadachowska-Brzyska, K., C. Li, L. Smeds, G. Zhang, and H. Ellegren. 2015. Temporal dynamics of avian populations during Pleistocene revealed by whole-genome sequences. Curr. Biol. 25:1375–1380.

Narasimhan, V., P. Danecek, A. Scally, Y. Xue, C. Tyler-Smith, and R. Durbin. 2016. BCFtools/RoH: a hidden Markov model approach for detecting autozygosity from next-generation sequencing data. Bioinformatics 32:1749–1751.

576 Napolitano, M.F., R. J. DiNapoli, J. H. Stone, M. J. Levin, N. P. Jew, B. G. Lane, J. T.
577 O'Connor, S. M. Fitzpatrick. 2019. Reevaluating human colonization of the Caribbean
578 using chronometric hygiene and Bayesian modeling. Sci. Adv. 5:eaar7806
579 Nielsen, R., T. Korneliussen, A. Albrechtsen, Y. Li, and J. Wang. 2012. SNP calling, genotype
580 calling, and sample allele frequency estimation from new-generation sequencing data.
581 PLOS ONE 7:e37558.
582 Pacala, S., and J. Roughgarden. 1982. Resource partitioning and interspecific competition in two
583 two-species insular *Anolis* lizard communities. Science 217:444–446.
584 Pacala, S. W., and J. Roughgarden. 1985. Population experiments with the *Anolis* lizards of St.
585 Maarten and St. Eustatius. Ecology 66:129–141.
586 Patton, A. H., L. J. Harmon, M. del R. Castañeda, H. K. Frank, C. M. Donihue, A. Herrel, and J.
587 B. Losos. 2021. When adaptive radiations collide: different evolutionary trajectories
588 between and within island and mainland lizard clades. Proc. Natl. Acad. Sci. 118.
589 Petkova, D., J. Novembre, and M. Stephens. 2016. Visualizing spatial population structure with
590 estimated effective migration surfaces. Nat. Genet. 48:94–100.
591 Petrenko, J. A., P. R. Martin, R. E. Fanelli, and F. Bonier. 2024. Urban tolerance does not protect
592 against population decline in North American birds. Biol. Lett. 20:20230507.
593 Powell, R. 2006. Conservation of the herpetofauna on the Dutch Windward Islands: St.
594 Eustatius, Saba, and St. Maarten. Appl. Herpetol. 3:293–306.
595 Powell, R., M. Dewynter, J. C. Daltry, and D. L. Mahler. 2020. *Anolis pogus*. International
596 Union for the Conservation of Nature Red List of Threatened Species
597 Powell, R., R. W. Henderson, and J. S. Parmerlee. 2005. The reptiles and amphibians of the
598 Dutch Caribbean : St Eustatius, Saba, and St Maarten.

599 Renjifo, L. M. 2001. Effect of natural and anthropogenic landscape matrices on the abundance of
600 subandean bird species. Ecol. Appl. 11:14–31.
601 Richardson, J. L., M. C. Urban, D. I. Bolnick, and D. K. Skelly. 2014. Microgeographic
602 adaptation and the spatial scale of evolution. Trends Ecol. Evol. 29:165–176.
603 Russell, J. C., and C. Kueffer. 2019. Island biodiversity in the Anthropocene. Annu. Rev.
604 Environ. Resour. 44:31–60.
605 Savary, P., J.-C. Foltête, H. Moal, G. Vuidel, and S. Garnier. 2021. graph4lg: A package for
606 constructing and analysing graphs for landscape genetics in R. Methods Ecol. Evol.
607 12:539–547.
608 Schwartz, A., and R. W. Henderson. 1991. Amphibians and Reptiles of the West Indies:
609 Descriptions, Distributions, and Natural History. University Press of Florida, Gainesville.
610 Scotti, I., H. Lalagüe, S. Oddou-Muratorio, C. Scotti-Saintagne, R. Ruiz Daniels, D. Grivet, F.
611 Lefevre, P. Cubry, B. Fady, S. C. González-Martínez, A. Roig, I. Lesur-Kupin, F.
612 Bagnoli, V. Guerin, C. Plomion, P. Rozenberg, and G. G. Vendramin. 2023. Common
613 microgeographical selection patterns revealed in four European conifers. Mol. Ecol.
614 32:393–411.
615 Selwood, K. E., M. A. McGeoch, and R. Mac Nally. 2015. The effects of climate change and
616 land-use change on demographic rates and population viability. Biol. Rev. 90:837–853.
617 Shaw, K. L., and R. G. Gillespie. 2016. Comparative phylogeography of oceanic archipelagos:
618 Hotspots for inferences of evolutionary process. Proc. Natl. Acad. Sci. 113:7986–7993.
619 Shchur, V., T. S. Korneliussen, and R. Nielsen. 2017. ngsPSMC: genotype likelihood-based
620 PSMC for analysis of low coverage NGS. (https://github.com/ANGSD/ngsPSMC)

621 Slatkin, M. 1993. Isolation by distance in equilibrium and non-equilibrium populations.
622 Evolution 47:264–279.
623 Slatkin, M., and R. R. Hudson. 1991. Pairwise comparisons of mitochondrial DNA sequences in
624 stable and exponentially growing populations. Genetics 129:555–562.
625 Steinbauer, M. J., R. Otto, A. Naranjo-Cigala, C. Beierkuhnlein, and J.-M. Fernández-Palacios.
626 2012. Increase of island endemism with altitude – speciation processes on oceanic
627 islands. Ecography 35:23–32.
628 Tolley, K. A., J. C. Groeneveld, K. Gopal, and C. A. Matthee. 2005. Mitochondrial DNA
629 panmixia in spiny lobster *Palinurus gilchristi* suggests a population expansion. Mar.
630 Ecol. Prog. Ser. 297:225–231.
631 Verboom, G. A., N. G. Bergh, S. A. Haiden, V. Hoffmann, and M. N. Britton. 2015. Topography
632 as a driver of diversification in the Cape Floristic Region of South Africa. New Phytol.
633 207:368–376.
634 Vieira, F. G., F. Lassalle, T. S. Korneliussen, and M. Fumagalli. 2016. Improving the estimation
635 of genetic distances from next-generation sequencing data. Biol. J. Linn. Soc. 117:139–
636 149.
637 Wang, I. J. 2013. Examining the full effects of landscape heterogeneity on spatial genetic
638 variation: a multiple matrix regression approach for quantifying geographic and
639 ecological isolation. Evolution 67:3403–3411.
640 Wang, I. J. 2009. Fine-scale population structure in a desert amphibian: landscape genetics of the
641 black toad (*Bufo exsul*). Mol. Ecol. 18:3847–3856.
642 Wang, I. J., and G. S. Bradburd. 2014. Isolation by environment. Mol. Ecol. 23:5649–5662.

643 Wang, I. J., R. E. Glor, and J. B. Losos. 2013. Quantifying the roles of ecology and geography in
644 spatial genetic divergence. Ecol. Lett. 16:175–182.
645 Wogan, G. O. U., M. L. Yuan, D. L. Mahler, and I. J. Wang. 2020. Genome-wide epigenetic
646 isolation by environment in a widespread *Anolis* lizard. Mol. Ecol. 29:40–55.
647 Wright, S. 1943. Isolation by distance. Genetics 28:114–138.
648 Young, A., T. Boyle, and T. Brown. 1996. The population genetic consequences of habitat
649 fragmentation for plants. Trends Ecol. Evol. 11:413–418.
650 Young, M., and M. H. Carr. 2015. Application of species distribution models to explain and
651 predict the distribution, abundance and assemblage structure of nearshore temperate reef
652 fishes. Divers. Distrib. 21:1428–1440.
653 Yuan, M. L., S. H. Dean, A. V. Longo, B. B. Rothermel, T. D. Tuberville, and K. R. Zamudio.
654 2015. Kinship, inbreeding and fine-scale spatial structure influence gut microbiota in a
655 hindgut-fermenting tortoise. Mol. Ecol. 24:2521–2536.
656 Yuan, M. L., J. H. Frederick, J. A. McGuire, R. C. Bell, S. R. Smith, C. Fenton, J. Cassius, R.
657 Williams, I. J. Wang, R. Powell, and S. B. Hedges. 2022. Endemism, invasion, and
658 overseas dispersal: the phylogeographic history of the Lesser Antillean frog,
659 *Eleutherodactylus johnstonei*. Biol. Invasions 24:2707–2722.
660 Yuan, M. L., C. Jung, J. H. Frederick, C. Fenton, K. de Queiroz, J. Cassius, R. Williams, I. J.
661 Wang, and R. C. Bell. 2023. Parallel and non-parallel phenotypic responses to
662 environmental variation across Lesser Antillean anoles. Evolution 77:1031–1042.
663 Zanaga, D., R. Van De Kerchove, D. Daems, W. De Keersmaecker, C. Brockmann, G. Kirches,
664 J. Wevers, O. Cartus, M. Santoro, S. Fritz, M. Lesiv, M. Herold, N. E. Tsendbazar, P. Xu,
665 F. Ramoino, and O. Arino. 2022. ESA WorldCover 10 m 2021 v200. Zenodo.
666

667 **Fig 1** (A) Boxplots of importance for each variable in our full random forest models. Minimum,
668 mean, and maximum null values are also shown. Variables are colored by importance
669 assessment: green – important, yellow – marginally important, and orange – not important. (B)
670 Predicted abundance across the landscape of St. Martin based on important variable (canopy
671 cover + elevation + urbanization) random forest model. Abundance survey plots are shown as
672 magenta points. (C) Predicted abundance across St. Martin based on GLM.

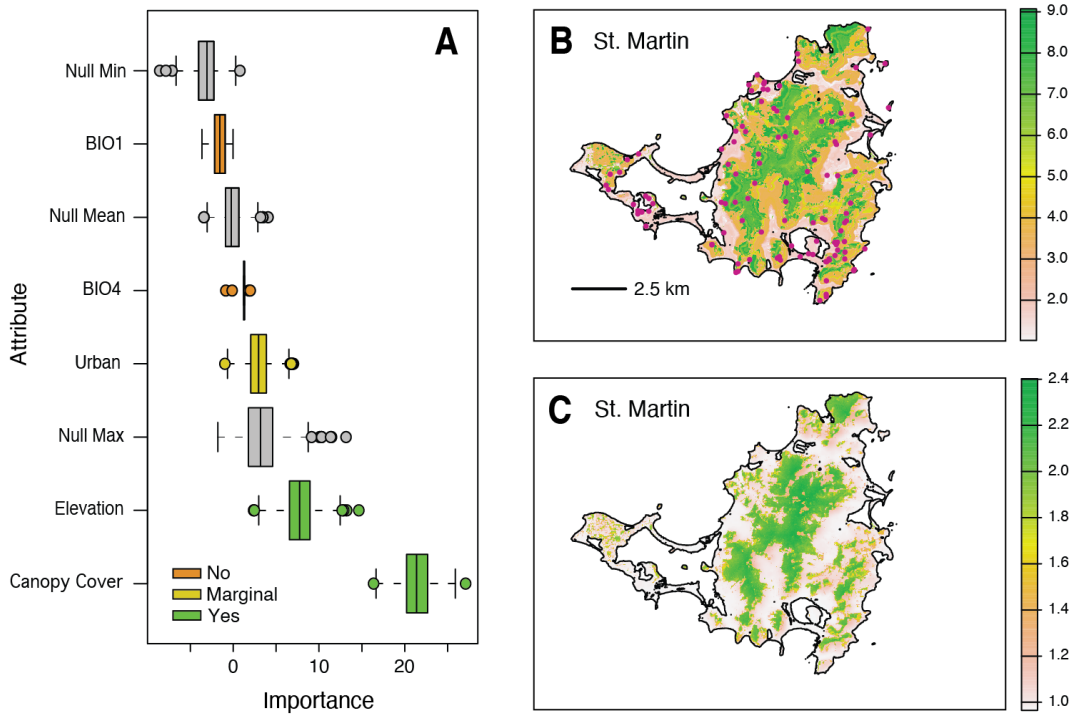

673

674

Fig 2 Above: PCA and MDS plots generated from WGS data for *A. pogus* sampled throughout the island of St. Martin. Individuals are labeled by collecting locality which corresponds to the map below. Below: dated mitogenome phylogeny of *A. pogus* on the island of St. Martin. Tips are connected to sampling locality on a canopy cover map of St. Martin. Nodes with a posterior probability above 0.98 are denoted by grey circles.

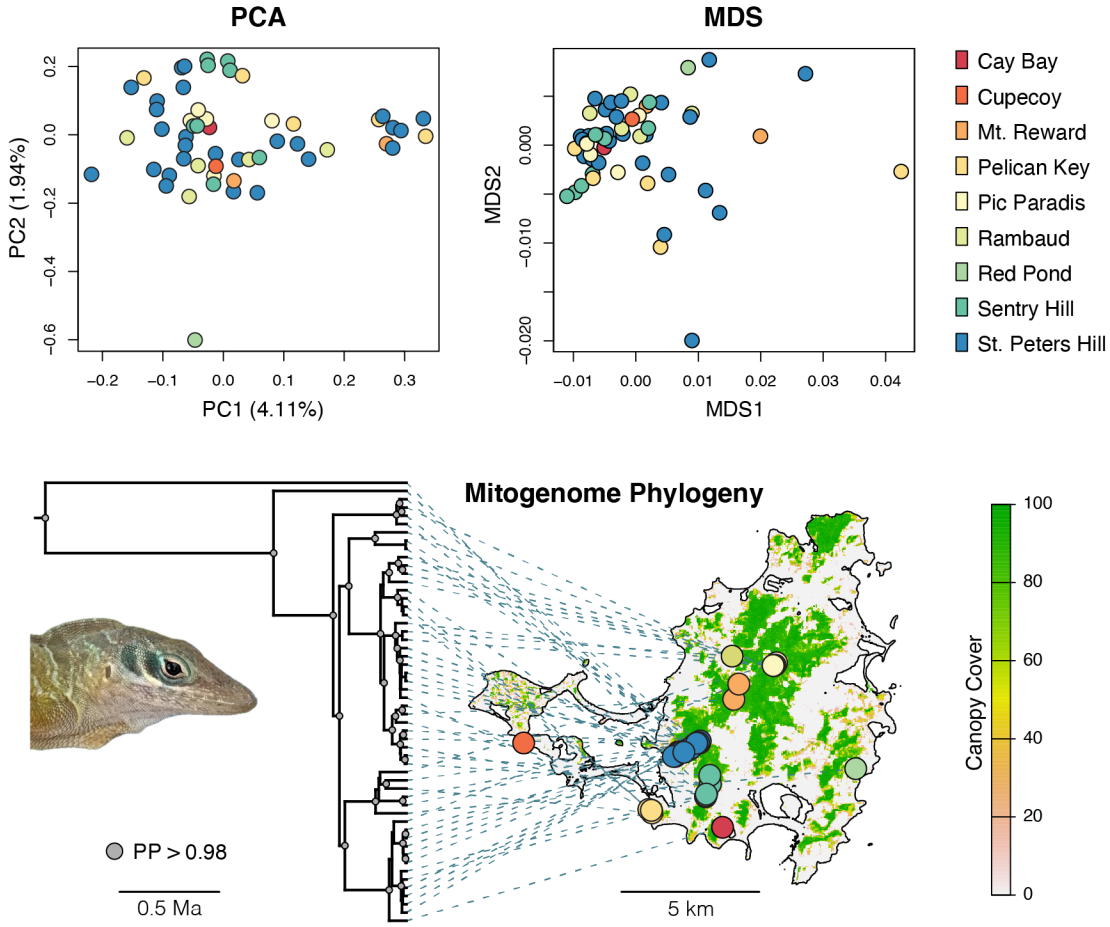

682 **Fig 3** (A) Inferred demographic history from ngsPSMC for *A. pogus* and *A. gingivinus*. For *A.*

683 *gingivinus* overall demographic patterns are consistent between Anguilla and St. Martin. Events

684 of potential interest (European arrival, human arrival, and the LGM) are denoted. (B)

685 Relationship between genetic and geographic distance including the 95% confidence interval as

686 determined by *graph4lg* for *A. pogus* on St. Martin. Geographic distance is shown in meters.

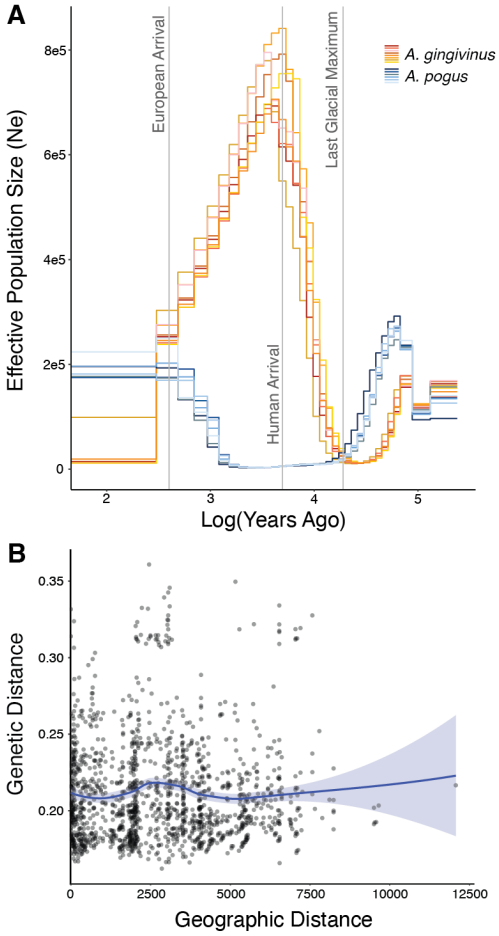

687

688 **Table 1** MMRR models of correlations between either (I) genomic or (II) mitogenomic distance
689 with geographic and environmental distances. Environmental variables tested are canopy cover,
690 elevation, urbanization, mean annual temperature (BIO1), and isothermality (BIO4). For each
691 model, individual coefficients and P-values for each predictor variables are shown.

I. Genomic		
	Coeff	*P*
Geographic	-0.073	0.602
Canopy Cover	-0.037	0.468
Elevation	-0.060	0.650
Urbanization	0.149	0.114
Annual Temperature	-0.069	0.662
Isothermality	0.107	0.412
II. Mitogenomic		
	Coeff	*P*
Geographic	-0.031	0.807
Canopy Cover	0.035	0.353
Elevation	-0.024	0.686
Urbanization	0.014	0.831
Annual Temperature	-0.048	0.699
Isothermality	0.027	0.746

692

693

Fig S1 Results from NGSadmix for *A. pogus*. Left: plot of ΔK for values of K between 2 and 6. The best fit K = 5. Right: admixture plots for K = 4, K = 5, and K = 6. Each bar represents a single individual and the proportion of ancestry assigned to each genetic deme. Individuals from the same sampling locality are denoted by the bars below the plots.

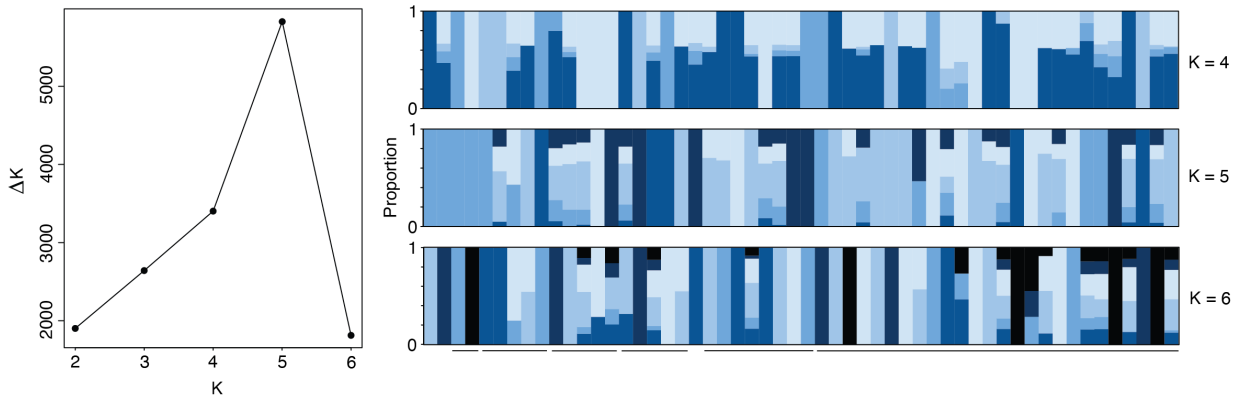

Fig S2 Estimated Effective Migration Surface (log migration) for *A. pogus* across the island of St. Martin. Gridded surface used for estimates are shown. Grey points represent samples scaled to sample size. Overall migration is low across the landscape.